JOURNAL OF MATERIALS SCIENCE 21 (1986) 444–450

Crystal chemistry of the $NaZr_2(PO_4)_3$, NZP or CTP, structure family

JAMES ALAMO*, RUSTUM ROY
Materials Research Laboratory, The Pennsylvania State University, University Park, Pennsylvania 16802, USA

The $NaZr_2(PO_4)_3$ type structure (abbreviated as NZP or CTP, $CaTi_4(PO_4)_6$), has emerged as a new family, which has extraordinary technological utility in three fields: fast-ion conductors, radwaste solidification and zero expansion ceramics. NZP or CTP is formed by an extraordinary range of discrete compositions and crystalline solutions. In this paper these compositions are classified according to their crystal chemical substitution scheme, and some uncommon trends in the systematic variation of their lattice parameters are shown. Some of the major trends are explained by correlation with the rotation of polyhedra in the structure.

1. Introduction

$NaZr_2(PO_4)_3$ (NZP), is the best known member of a very large family of compounds and crystalline solutions that has been intensively studied just in the last 15 years. The crystal structure was solved first for the $NaZr_2(PO_4)_3$ composition and the titanium and germanium analogues in 1968 by Hagman and Kierkegaard [1]. In the following year in Yugoslavia, the crystal structure of $KZr_2(PO_4)_3$ [2] was presented as a representative for all the alkali zirconium or hafnium double phosphates, that had been reported previously to be isomorphous [3, 4]. Later on, still more phosphates and anhydrous sulphates were shown to be isomorphous with NZP, this time in France [5–8].

The NZP phase is hexagonal and remains stable through a wide variation in atomic parameters as well as in the number of extra occupancies or vacancies. In 1976, Hong [9] and Goodenough *et al.* [10] brought the world's attention to the fact that the substitution of P^{5+} for $Si^{4+} + Na^+$ in a stuffing site in NZP makes this structure exhibit "super-ionic" conductivity. They also showed how the structure can suffer a monoclinic distortion without breaking any bonds. Following this finding, a very wide variety of chemical substitutions, syntheses and structural studies have been attempted to improve this ionic transport property (just a sample of the papers written are given [11–31]).

In these wide-ranging studies, some of the boundaries of the parent structure fields are trespassed and new distortions of the structrue are discovered.

In the eighties, in addition to the fast-ion transport property two other remarkable properties of the same structure were discovered in this laboratory. Roy *et al.* [32, 33] showed that NZP is unique in its capability to accommodate all the ions present in the normal fuel reprocessing stream and form a single-phase ceramic radiophase. The accommodation of the different radionuclides in the different sites occurs as shown below. In a separate series of papers the present authors and their colleagues also showed that these materials constitute an ideal ceramic family for controlled near-zero thermal expansion [34–36]. Fig. 1 shows the thermal expansion of representative compositions, and Fig. 2 shows how the net near-zero values of volume expansion are attained via the crystalline anisotropy in linear expansivity, α.

The present paper is an attempt to bring together the diverse structural and compositional data accumulated so far.

2. The structure

Fig. 3 shows the structure of NZP. The strongest bonds in the NZP strucure are, of course, around phosphorus and zirconium atoms, which form quite rigid polyhedra with the oxygen. The PO_4 and ZrO_6 groups form nearly regular tetrahedra and octahedra respectively, and they are connected (sharing corners only) in such a way that they build up a flexible but stable skeleton. Sodium atoms fill in certain other octahedral holes. The basic structural unit from which the whole structure can be understood is shown in Fig. 3a. It is shown aligned with the [0 0 1] direction, and repetitive units are seen to build up a chain whose projection is shown in Fig. 3b. Chains are packed hexagonally (Fig. 4), and connected through the phosphate groups to the sodium polyhedra in the neighbouring chains yielding a true rhombohedral cell with space group $R\bar{3}c$.

The $[Zr_2(PO_4)_3]^{-1}$ skeletons create three important kinds of "holes" as they are articulated: into the final crystal structure ($R\bar{3}c$), the octahedral one ($\bar{3}$) normally occupied by sodium, the prismatic one (32) formed by the phosphate, that is normally vacant, and three more octahedral ones ($\bar{1}$) that set up a three-dimensional network of channels and allow for the ionic conductivity.

---

*Present address: Department of Inorganic Chemistry, College of Chemistry, Valencia University, Burjasot, Spain.

0022–2461/86 $03.00 + .12

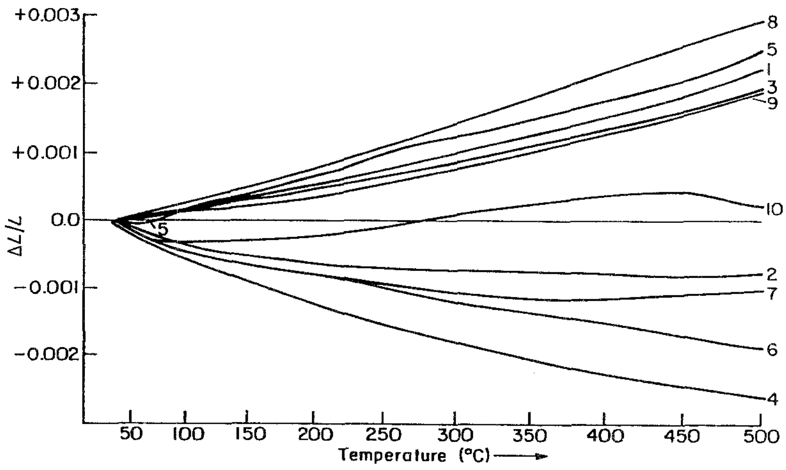

Figure 1 Thermal expansion of a variety of compositions each with the NZP structure. 1, $Ca_{0.5}Ti_2P_3O_{12}$; 2, $Ca_{0.5}Zr_2P_3O_{12}$; 3, $Ca_{0.5}ZrTiP_3O_{12}$; 4, $NaTi_2P_3O_{12}$; 5, $Na_3Cr_2P_3O_{12}$; 6, $NaZr_2P_3O_{12}$; 7, $Na_{3/2}Zr_{15/8}P_3O_{12}$; 8, $Ca_{0.25}Na_{0.5}Zr_2P_3O_{12}$; 9, $Ca_{0.25}Na_{0.5}Ti_2P_3O_{12}$; 10, $Na_{1.5}Zr_{1.5}Cr_{0.5}P_3O_{12}$.

3. Range of ionic substitution

The standard formula for this structure may be written

$$M_1'^{X} M_3''^{VI} A_2^{VI} B_3^{IV} O_{12}$$

The truly remarkable richness of the ionic substitutions which has been achieved in this structure is due to the M′ and M″ sites which are the holes or vacancies formed by the rather strong skeleton and which can be left vacant with no effect on the crystallography of the structure. The several different classes of substitution which we will discuss in the subsequent presentation may be summarized as follows starting with the $NaZr_2P_3O_{12}$ composition as the parent. (Only one example of the ions which are substituted is shown for simplicity.) The reader will find in the tables that each such ion represents many other with similar ionic radius.

Isovalent substitution in M′ site	Na^+ Rb	$[\ ]_3$ –	Zr_2^{VI} –	P_3^{IV} –	O_{12} –
Isovalent substitution in VI fold	–	–	Sn_2^{4+}	–	–
Balanced substitution VI and IV	–	–	$Ta^{5+}Zr^{4+}$	$Si^{4+}P_2^{5+}$	–
Ditto between IV fold site and M′	–	Na^+	–	$Si^{4+}P_2^{5+}$	–
Ditto between IV fold site and M′	–	Na_2^+	–	$Si_2^{4+}P^{5+}$	–
Heterovalent substitution sites within M sites	$Ca_{0.5}[\ ]_{0.5}$	–	–	–	–
Balanced substitution between M′ and other sites	$[\ ]_1$ $[\ ]_1$	– –	$Ta^{5+}Zr^{4+}$	– $P_2^{5+}S^{6+}$	– –

The substitutions can be complete (as shown in the examples above) or partial, leading to crystalline solutions of any intermediate composition. The range of ions which have been introduced in substantial (greater than say 0.33 atom fraction) in each site or in the various combinations as shown in the different schemes above, are listed below.

M′	M″	A	B
↓	↓	↓	↓
Li, Na, K, Rb, Cs, Mg, Ca, Sr, Ba	Na, K	Sn, Ge, Ti, Zr, Hf, Al, Cr, Nb, Ta, Sc	P, Si, Al, S

4. Analysis of crystal chemical relations

We have extracted from the literature the crystallographic data available on the many phases studied, and added to this data set, our own measurements made on many phases we have prepared ourselves. Wherever ionic radii are plotted we have used the Shannon and Prewitt [37] data as added to by Muller and Roy [38].

Next we have studied the relationship between composition and lattice parameters in some detail. As may be expected the relationship depends upon the several crystal chemical particularities, and general correlations over all kinds of substitutions at the same time are not possible. We therefore treat each simple substitution in turn.

4.1. The effect of composition on lattice parameters

Fig. 5 first shows a plot of *c* against *a* for the phosphates in the first substitutional group. The two trends apparent in this plot are: first, for the same M′, the larger the A atom, the larger are *a* and *c*. Second, for the same A atom, the larger the M′, the larger is *c* but the *smaller* is *a*. The first trend sounds normal, i.e. substitution of an A atom by a larger cation expands the structure. The second appears anomalous, i.e. substitution of M′ by a larger cation makes the structure expand in the *c* direction but to *contract* in the *a* direction.

Data found in the literature about sulphates falling in the first substitutional group correspond to compounds containing always sodium in the M′ position, at the same time that A positions are filled with a pair

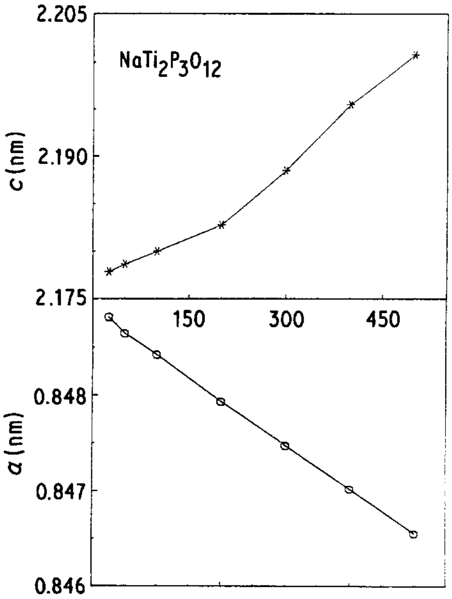

Figure 2 Anisotropy of thermal expansion of $NaTi_2P_3O_{12}$ determined by high-temperature X-ray diffraction.

of different cations. Hence simple calculations cannot be made in these cases. Instead, a distribution of points is spread around the "sodium line" (Fig. 6).

Data corresponding to the second substitutional group, i.e. those in which the M′ position is vacant, give an analogous distribution to the former one so the "sodium line" and the "vacant line" are almost coincident. Both are plotted together in Fig. 6. It would appear that the size of the M′ hole in the unoccupied skeleton is nearly the same as that required by the sodium atom.

Most of the compounds in the third substitutional group, i.e. those in which the M″ holes are also filled, have been studied because of their potential ionic conductivity, adding two more Na^+ at the time that two P^{5+} or two Zr^{4+} are substituted by two Si^{4+} or two M^{3+} respectively, so they match one of the following formulae: $Na_3Zr_2(SiO_4)_2(PO_4)$ or $Na_3M_2^{3+}(PO_4)_3$.

Only a few more examples appear in this group with other monovalent cations (lithium, potassium, silver) instead of sodium, and only one example shows complete filling of the holes, $Na_4Zr_2(SiO_4)_3$. So, the crystal chemical trends are limited. In Fig. 7, the lattice parameters of these compounds are plotted together with their crystalline solutions with $NaZr_2(PO_4)_3$, and on it is traced the locus for the tervalent substituted compounds. This line shows the same slope as that of the "sodium line" in Fig. 6, but it is shifted. The points representing each compound are distributed along the line according to the size of the tervalent cations. The points for the crystalline solutions show that the changes in the lattice parameters are linear for the smaller cations, being more and more non-linear for the ytterbium (Yb) and the yttrium (Y) case.

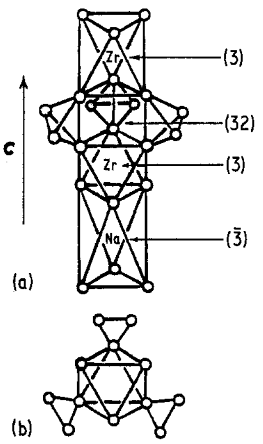

Figure 3 Idealized basic structural unit for $NaZr_2(PO_4)_3$ structure. (a) Repetitive set of polyhedra in the [0 0 1] direction. The site symmetry on the central axis is in parentheses. The oxygens in sodium-polyhedra come from PO_4 in neighbouring chains. (b) Projection of the basic unit.

The most interesting fact is that although the scandium (Sc) and indium (In) cations have nearly the same size as Zr^{4+}, parameter a for the substituted compounds is bigger but parameter c is smaller. This clearly means that the extra sodium incorporated in the structure is responsible for this anomalous change. Although the same cause must be in effect in all the other similar compounds, the simultaneous change in the size of the A cation makes the correlation not so obvious.

4.2. The boundaries

The plots in Figs. 5 to 7 are not the detailed structure field maps in radius space (see for example the text by Muller and Roy [38]). The plots accept only hexagonal or pseudo-hexagonal a and c parameters to plot a point, these are related to the size of cations in the structure. Hence the boundaries of the NZP field will appear not as the non-existence of the structure and competitive structures appear as new compounds. The stability of the hexagonal phase decreases slightly in some of the compounds plotted in boundaries in such a way that they suffer a small atomic displacement decreasing the symmetry to monoclinic. This effect appears particularly when the M′ position is vacant, as in $Zr_2(PO_4)_2(SO_4)$, $ZrNb(PO_4)_3$, or also $Na_3Zr_2(SiO_4)_2(PO_4)$, where the sodium population appears to be mostly in M″ positions. Nevertheless, the free energy for these structures must be very close, as some compounds are known in several phases such as $Na_3Sc_2(PO_4)_3$ with one hexagonal [30], and two monoclinic [16, 17] structures, one showing the antidisplacement of the other. Others show one or more reversible displacements, e.g. $Na_3Sc_2(PO_4)_3$ or $Na_3Zr_2(SiO_4)_2(PO_4)$.

In addition to these closely related phases, several other structures appear beyond the stability boundaries. For bigger A cations such as uranium and thorium, the coordination number must change from 6 to 9 [4]. In the case of tervalent, cerium, neodymium and praseodymium, the structure is also different [39]. Monazite is a very stable and competitive structure. $KTi_2(PO_4)_3$ appears also with the $K_2Mg_2(SO_4)_3$ structure in which one potassium is missing [5].

4.3. Mechanisms of internal adjustment of the structures

The substitutions described above yield lattice changes that may be classified as normal or non-normal. Normal or expected changes, such as the expansion of a and c when A is bigger, needs no explanation. The A

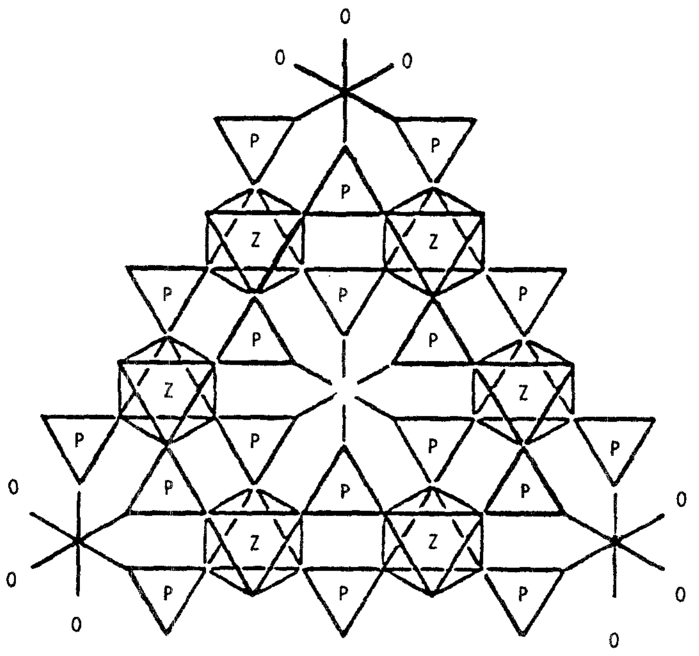

Figure 4 Hexagonal packing of chains. The central chain is shifted $\frac{1}{3}c$.

cation is the one creating the skeleton and the dimensions of which are proportional to the size of A. On the other hand, the understanding of other changes requires an explanation, that is based on *distortions* suffered by the *skeleton*. Unfortunately for this purpose, only a few single crystals have been studied by X-ray diffractometry and only in three cases have the atomic coordinates been published. So detailed evidence for the atomic displacements after substitutions is not available in the literature. However, based on these data, the detailed powder work we have done on many samples and other insights into the structure have suggested several possible explanations for these changes. Extensive calculations rejected some of our earlier proposed models.

The final model which survived appears to explain most of these facts:

1. the skeleton can modify itself to accomodate small as well as large cations in M′ holes, such as (Li, H, or Cs)$^+$ [3, 24];
2. in order to increase the size of the M′ holes this flexible skeleton contracts in the *a* direction and expands in the *c* direction;
3. in order to accomodate extra ions in the M″ holes the skeleton contracts in the *c* direction and expands in the *a* direction, just in the opposite way expressed in the second point, so tensions appear in the structure

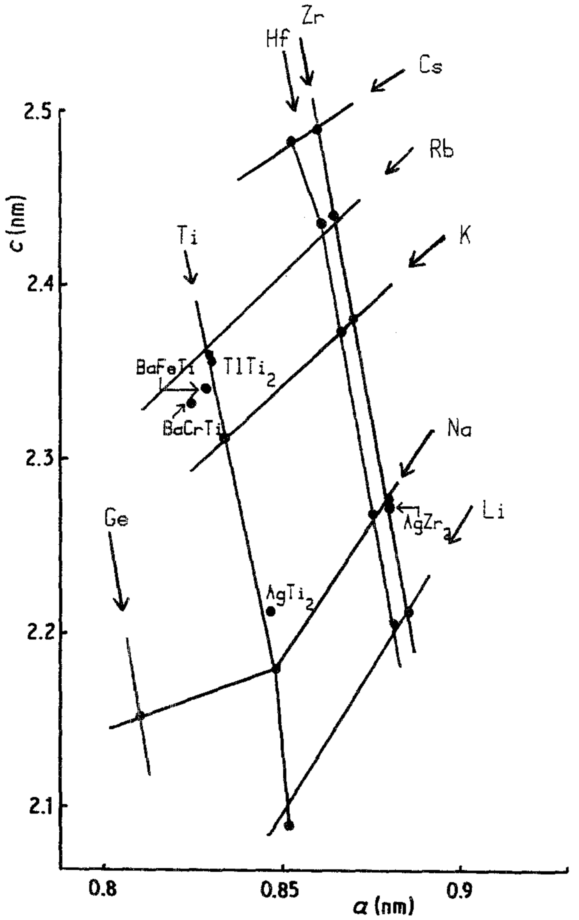

Figure 5 A plot of lattice parameters *c* against *a* for M′A$_2$(PO$_4$)$_3$ where A = (Ge, Ti, Hf, Zr) and M′ = (Li, Na, K, Rb, Cs, Tl, Ag).

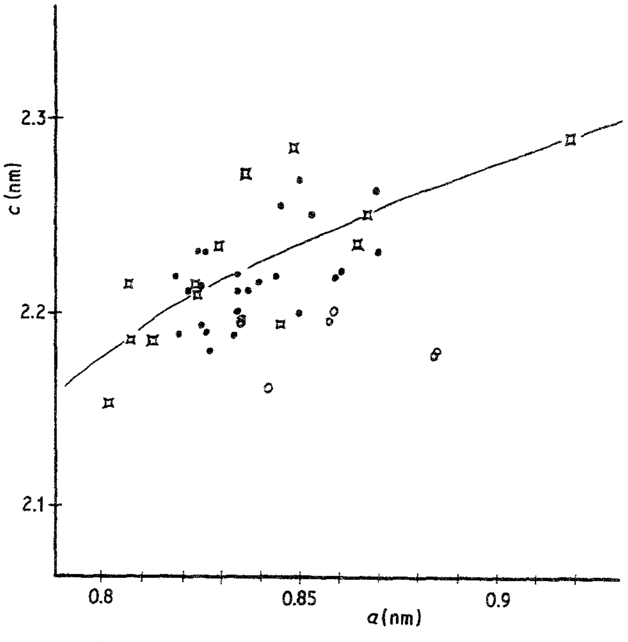

Figure 6 A plot of lattice parameters *c* against *a* for ● NaAA^1(SO$_4$)$_3$ where A = (Mg, Co, Ni, Zn, Mn) and A^1 = (Al, Ga, In, Cr, Fe), ¤ A$_2$(SO$_4$)$_3$ where A = (Y, In, Sc, Rh, Ga, Cr, V, Fe, Ti, Al), and ○ AA^1(PO$_4$)$_3$ where A = (Ti, Ge, Zr) and A^1 = (Sb, Nb, Ta).

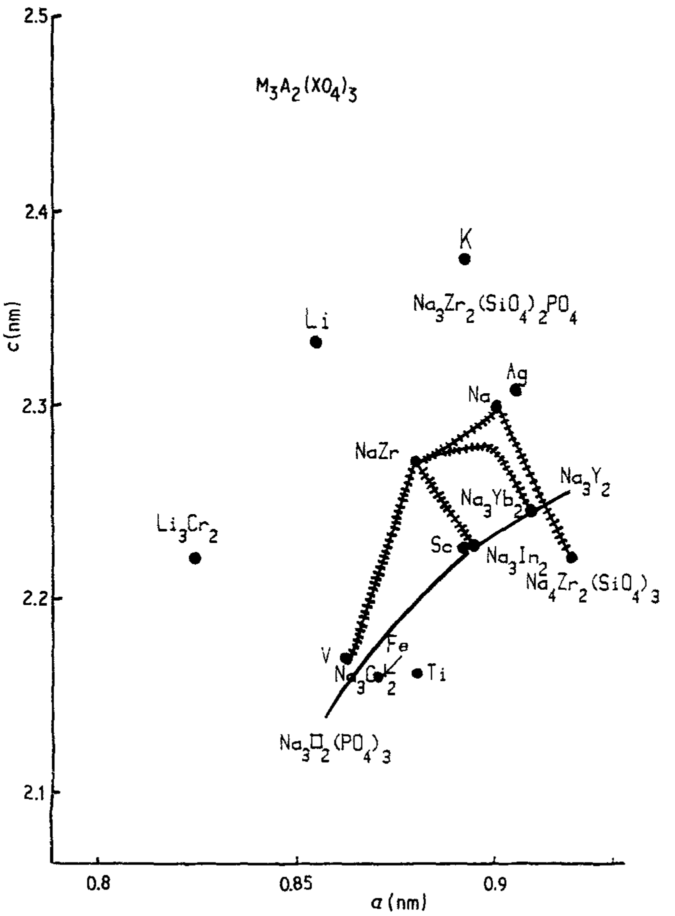

Figure 7 A plot of lattice parameters c against a for $M'_3A_2(XO_4)_3$ where M′ = (Li, Na, K, Ag), A = (Zr, Cr, Fe, Ti, Y, V, Sc, In, Yb) and X = (P, Si) and in some cases their crystalline solutions with $NaZr_2(PO_4)_3$.

making the cations in M′ jump to M″ [27], and also to distort to the monoclinic distribution.

The model is based in the singular fact that the skeleton is built up by PO_4 tetrahedra and ZrO_6 octahedra that share vertices so the bonds are very strong and the skeleton very stable, but at the same time these bonds can bend and here the polyhedra can show small rotations without breaking the structure. As a matter of fact, phosphorus and zirconium polyhedra in $NaZr_2(PO_4)_3$ [1] and $KZr_2(PO_4)_3$ [2] are already rotated in different degrees showing a dependence of this rotation on the size of the atom in the M′ position. Figs. 8 and 9 show the actual projections of $NaZr_2(PO_4)_3$.

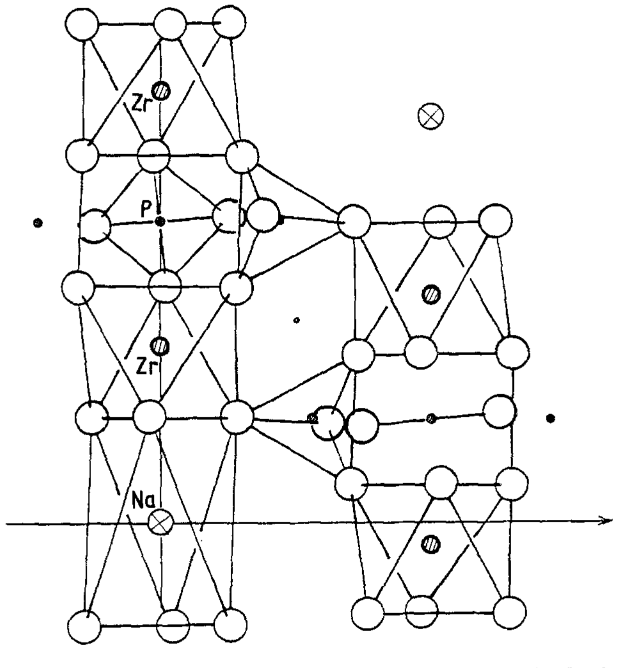

Figure 8 Partial projection of the $NaZr_2(PO_4)_3$ structure in the *b* direction.

In Figs. 10a and b, parts of the structure involved in the rotations are plotted to show their nature. None of these rotations break the existing symmetry in the unit cell, as phosphorus tetrahedra rotate around the two-fold axis and the zirconium octahedra around the three-fold axis.

The chains along the c-axis move closer when the phosphate groups rotate and so the structure contracts in the a direction. Simultaneously, the zirconium octahedra rotate alternately as shown in Fig. 10b to accommodate and maintain the P–O and Zr–O bonds. The quantitative effect can be more clearly visualized from Fig. 9.

The expansion in the c direction is also due to the phosphate rotations as can be easily noted in Fig. 8. The sodium atom is in (0 0 0) and the phosphorus atom is in (x, x, $\frac{1}{4}$) so their distance has a component in the c direction equal to $c/4$. Rotating the phosphorus tetrahedra, sodium and phosphorus are pushed apart and so the structure expands in the c direction. This expansion does not affect significantly the zirconium polyhedra and it is absorbed in the weakest part of the structure: the M′ hole. Other distortions appear in the prismatic hole that contracts in the c direction.

All rotations presented above can now be considered to take place in the opposite direction. The results on lattice parameters are just the opposite, i.e. the structure will expand in the a direction and it will contract in the c direction, at the same time the M′ hole will become smaller, at least until the prismatic

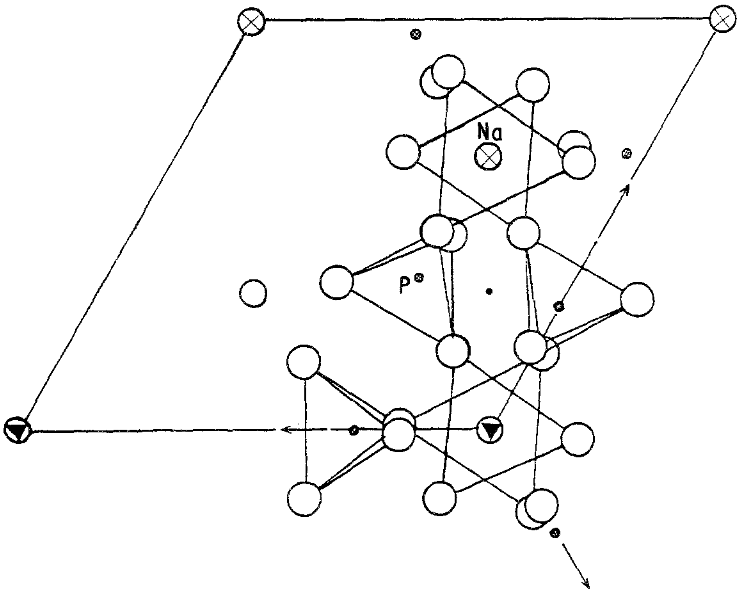

Figure 9 Projection of the same polyhedra as in Fig. 6, now in the *c* direction.

hole obtains perfect *3/mm* symmetry, then a different effect shows up but no compound seems to illustrate this last situation.

Following the preceding discussion it can now be understood how the skeleton can accomodate itself to almost any size of cation occupying the M′ hole, from Li^+ to Cs^+. Moreoever, this also helps to explain the extraordinary fact that changing from lithium to caesium results in a unit cell which shows a *smaller a* and larger *c*.

A computer program based on this model and keeping constant the bond distances in $NaZr_2(PO_4)_3$ [1] for P–O and Zr–O was used to solve the equations for a number of progressive rotations of the polyhedra. The calculated *a* and *c* are plotted in Fig. 11 together with those for the Li–Cs series. The model appears to be very effective assuming that the zirconium octahedra can be expected to be somewhat different from the lithium to the caesium compound.

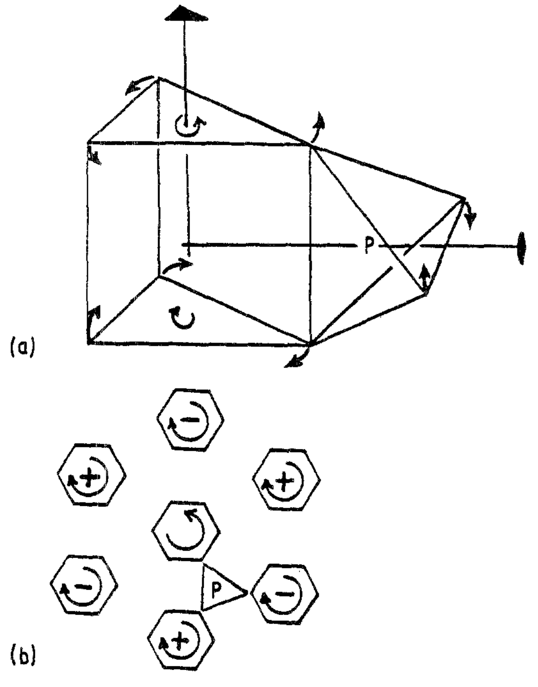

Figure 10 (a) and (b) Rotation of oxygens around the three- and two-fold axis to accommodate the skeleton to the structural requirements in each compound.

These highly anomalous changes of *a* and *c* caused by increasing the radius in the M′ sites can now be seen to have foreshadowed the most interesting anomalous thermal expansion properties which we have demonstrated (see Figs. 1 and 2) with the composition held constant and only temperature increased.

A third point which our model explains is that the M″ holes lie between every two vertical chains; hence filling them with cations will cause the structure to expand in the *a* direction, making the M′ hole smaller and forcing atoms there to jump out, and in the limit, distorting the structure to monoclinic symmetry and causing *c* to decrease.

For the other cases in which zirconium is substituted for by chromium, scandium or yttrium, or phosphorus by silicon, sulphur or silver, for example, an additional parameter must be taken into account, i.e. the overall change of the skeleton due to the new size of its constitutional parts. These effects may be dominant and have been discussed before and classified as normal or expected changes.

5. Conclusions

We have shown that the $NaZr_2(PO_4)_3$-type structure is remarkably stable towards ionic substitution, supporting a vast range of homovalent, as well as heterovalent substitutions because of the flexibility of its skeleton, the strength of its bonds, and the existence of a variety of holes that can stay vacant or occupied as well.

Every atom can be substituted by others playing analogous crystal chemistry roles. The M′ holes can be filled by monovalent or divalent cations, but no tervalent ions have been reported to appear in this position and only one tetravalent in $Zr_{1/4}Zr_2(PO_4)_3$ that is less stable than the other compounds with the same chemical skeleton [40]. The M″ holes have been filled normally by alkali cations. The A atom has been substituted by a ter-, tetra- or pentavalent one, but never a lesser charged ion. Finally, the X atom can be a tetra-, penta- or hexavalent ion.

The better understanding of the crystal chemistry of this structure will, we believe, help to prepare more compounds and to determine the precise stability

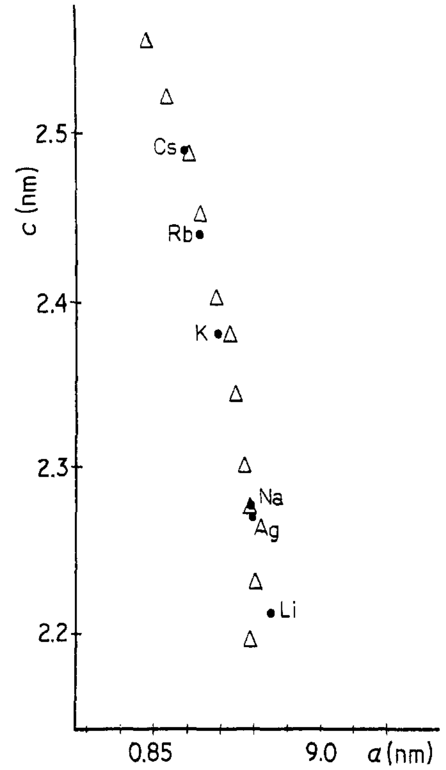

Figure 11 A plot of lattice parameters *c* against *a* in $MZr_2(PO_4)_3$. ● M = (Li, Ag, Na, K, Rb, Cs), together with those (△) generated by computer.

limits of the structures. Those limits for the transition to the monoclinic distortion when M′ is vacant, or with a very small cation, or when it is forced to jump to the M″ holes, depend both on the temperature and on the exact stoichiometry of phases.

The coordinated rotations of the tetrahedra and octahedra that constitute the skeleton are responsible for the opposed changes in the lattice parameters, when substituting the M′ cation or when filling new atoms into the M″ holes, keeping constant the size of the skeleton. *These* changes are parallel to the changes caused by temperature and account for the near-zero thermal expansion values for some compositions.

Substitution of the skeleton polyhedra makes the same proportional change in both lattice parameters.

Acknowledgements

We wish to thank H. A. McKinstry for his enthusiasm and help with the computer calculations carried out on an Apple II plus. This research was completed with the help of support from Grant no. AFOSR-83-0291.

References

1. L. HAGMAN and P. KIERKEGAARD, *Acta Chem. Scan.* **22** (1966) 1822.
2. M. SLJUKIC, B. MATKOVIC, B. PRODIC and D. ANDERSON, *Z. Kristallographie* **130** (1969) 148.
3. M. SLJUKIC, B. MATOVIC, P. PRODIC and S. SCARNICAR, *Croat. Chem. Acta* **39** (1967) 145.
4. B. MATOVIC, B. PRODIC and M. SLJUKIC, *Bull. Soc. Chim. Fr.* (1968) 177.
5. RENE MASSE, A. DURIF, J. C. GUITEL and I. TORDJMAN, *Bull. Soc. Fr. Min. Crist.* **95** (1972) 47.
6. RENE MASSE, *ibid.* **95** (1972) 405.
7. RENE MASSE, J. C. GUITEL and R. PERRET, *ibid.* **96** (1973) 346.
8. RENE PERRET, A. THRIERR-SOREL, J. P. PETER and R. MASSE, *ibid.* **98** (1975) 103.
9. H. Y. HONG, *Mater. Res. Bull.* **11** (1976) 173.
10. J. B. GOODENOUGH, H. Y. HONG and J. A. KAFALAS, *ibid.* **11** (1976) 203.
11. B. E. TAYLOR, A. D. ENGLISH and T. BERZINS, *ibid.* **12** (1977) 171.
12. C. DELMAS, R. OLAZCUAGA, F. CHERKAOUI, R. BROCHU and G. LE FLEM, *C. R. Acad. Sci. Paris* **287C** (1978) 169.
13. M. PINTARD-SCREPEL, F. d'YVOIRE and F. REMY, *ibid.* **286C** (1978) 381.
14. R. BROCHU, F. CHERKAOUI, C. DELMAS, R. OLAZCUAGA and G. L. FLEM, *ibid.* **298C** (1978) 85.
15. A. LA GINESTRA, C. FERRAGINA and P. PATRONO, *Mater. Res. Bull.* **14** (1979) 1099.
16. V. A. EFREMOV and V. B. KALININ, *Sov. Phys. Crystallogr.* **23** (1978) 393.
17. H. Y. HONG, in "Proceedings of the International Conference on Fast Ion Transport in Solids", 21 to 25 May 1979, Lake Geneva, edited by P. Vashishta, J. N. Mundy and G. K. Shenoy (Elsevier, North- Holland,) pp. 431–33.
18. D. TRANQUI, J. J. CAPPONI, J. C. JOUBERT, R. D. SHANNON and C. K. JOHNSON, *ibid.*, pp. 439–42.
19. U. VON ALPEN and M. F. BELL, *ibid.*, pp. 443–46.
20. G. R. MILLER, B. J. McENTIRE, T. D. HADNAGY, J. R. RASMUSSEN, R. S. GORDON and A. V. VIRKAR, *ibid.*, pp. 83–6.
21. U. VON ALPEN, M. F. BELL and W. WICHELHAUS, *Mater. Res. Bull.* **14** (1979) 1317.
22. J. P. BOILOT, J. P. SALANIE, G. DESPLANCHES and D. L. POTIER, *ibid.* **14** (1979) 1469.
23. D. H. H. QUON, T. A. WHEAT and W. NESBITT, *ibid.* **15** (1980) 1533.
24. A. CLEARFIELD, P. JIRUSTITHIPONG, R. N. COTMAN and S. P. PACK, *ibid.* **15** (1980) 1603.
25. M. NAGAI, S. FUJITSU and T. KANAZAWA, *J. Amer. Ceram. Soc.* **63** (1980) 476.
26. F. d'YVOIRE, M. PINTERD-SCREPEL and E. BRETEY, *C.R. Acad. Sci. Paris* **290C** (1980) 185.
27. C. DELMAS, J. C. VIALA, R. OLAZCUAGA, G. LE FLEM, P. HAGENMULLER, F. CHERKAOUI and R. BROCHU, *Mater. Res. Bull.* **16** (1981) 83.
28. C. DELMAS, R. OLAZCUAGA, G. LE FLEM, P. HAGENMULLER, F. CHERKAOUI and R. BROCHU, *ibid.* **16** (1981) 285.
29. A. CLEARFIELD, L. P. JERUS and R. N. COTMAN, *Solid State Ionics* **5** (1981) 301.
30. J. P. BOILOT, G. COLLIN and R. COMES, *ibid.* **5** (1981) 307.
31. B. O. HALL, *ibid.* **5** (1981) 317.
32. RUSTUM ROY, E. R. VANCE and JAMES ALAMO, *Mater. Res. Bull.* **17** (1981) 585.
33. RUSTUM ROY, LIJI YANG, JAMES ALAMO and E. R. VANCE, in "Proceedings of Scientific Basis for Nuclear Waste Management VI", edited by D. G. Brookins (Elsevier, New York, 1983) p.15.
34. JAMES ALAMO and RUSTUM ROY, *J. Amer. Ceram. Soc.* **63** (1984) C78.
35. JAMES ALAMO and H. A. McKINSTRY, in preparation.
36. RUSTUM ROY, D. K. AGRAWAL, JAMES ALAMO and R. A. ROY, *Mater. Res. Bull.* **19** (1984) 471.
37. R. D. SHANNON and C. T. PREWITT, *Acta Crystallogr.* **B25** (1969) 925.
38. OLAF MULLER and RUSTUM ROY, "The Major Ternary Structural Families" (Springer-Verlag, New York 1974) pp. 11–12.
39. A. I. KRYUKOVA, I. A. KORSHUNOV, E. P. MOSKVICHEV, V. A. MITROFANOVA, N. V. VORB'EVA, G. N. KAZANTSEV and O. V. SKIBA, *Russ. J. Inorg. Chem.* **21** (1976) 1408.
40. JAMES ALAMO and RUSTUM ROY, *J. Amer. Ceram. Soc.* **63** (1984) C80.

Received 5 February
and accepted 13 March 1985